Optimization of Postprocessing parameters for abdominal Forensic CT scans

Hansen, Pernille Lund; Leth, Peter Mygind; Nielsen, Pernille Aagaard; Bech, Dina Maria; Nielsen, Julie Brandhøj; Mørup, Svea Deppe; Holst, Anette Koch; Bak, Lene; Poulsen, Mette R.; Greisen, Pernille W.; Hansen, Dennis Lund; Precht, Helle

Published in:
Forensic Science International: Synergy

DOI:
10.1016/j.fsisyn.2024.100478

Publication date:
2024

Document version:
Final published version

Forensic Science International: Synergy 8 (2024) 100478

Contents lists available at ScienceDirect

Forensic Science International: Synergy

journal homepage: www.sciencedirect.com/journal/forensic-science-international-synergy

Optimization of Postprocessing parameters for abdominal Forensic CT scans

Pernille Lund Hansen [a,*], Peter Mygind Leth [b], Pernille Aagaard Nielsen [a], Dina Maria Bech [a], Julie Brandhøj Nielsen [a], Svea Deppe Mørup [a], Anette Koch Holst [c], Lene Bak [c], Mette R. Poulsen [c], Pernille W. Greisen [c], Dennis Lund Hansen [d,e], Helle Precht [a,f,g]

[a] Health Sciences Research Centre, University College Lillebaelt, Odense, Denmark
[b] Institute of Forensic Medicine, University of Southern Denmark, Odense, Denmark
[c] Department of Radiology, Odense University Hospital, Odense, Denmark
[d] Department of Hematology, Odense University Hospital, Odense, Denmark
[e] Department of Clinical Research, University of Southern Denmark, Odense, Denmark
[f] Department of Radiology, Lillebaelt Hospital, Kolding, Denmark
[g] Department of Regional Health Research, University of Southern Denmark, Kolding, Denmark

A R T I C L E I N F O

Keywords:
Postmortem computed tomography
Forensic pathology
Image quality
Diagnostic quality
Virtual autopsy
Virtopsy

A B S T R A C T

Aim: Postmortem Computed Tomography (PMCT) is gradually introduced at forensic institutes. Image reconstruction software can increase diagnostic potential in CT by increasing distinction between structures and reduction of artifacts. The aim of this study was to develop and evaluate novel image reconstruction parameters for postmortem conditions, to increase image quality and diagnostic potential of CT scans.
Method: Twenty PMCT scans of deceased hereof two in severe decay were subjected to four reconstruction techniques: a standard reconstruction algorithm, the detail reconstruction algorithm and two novel algorithms based on the standard algorithm, but with different Hounsfield settings. Image quality was evaluated by visual grading analysis (VGA) by four forensic radiologist observers.
Results: The VGA did not prove that any of the reconstruction techniques were superior to the others. For standard and detail, the two pre-defined reconstruction algorithms, VGA scores were indiscernible and were superior to the equally indiscernible Hounsfield reconstructions on parameters translated into Sharpness and Low Contrast Resolution. The two alternative Hounsfield settings were superior with respect to Noise and Artifacts/Beam Hardening.
Conclusion: The study elucidates the possiblity for multiple reconstructions specialized for PMCT conditions, to accommodate the special conditions when working with the deceased. Despite the lack of clear improvements in the tested reconstructions, this study provides an insight into some of the possibilities of improving PMCT quality using reconstruction techniques.

1. Introduction

Computed Tomography (CT) was developed as a tool to aid the diagnostic process of living patients [1]. As such, foci for development has been on diagnostic quality and reduction of radiation exposure and movement artifacts [2–4]. Throughout the last few decades, Postmortem Computed Tomography (PMCT) scans have become a tool used to supplement or in some cases to replace the autopsy [5–8]. Previous studies have found that postmortem CT is superior to Magnetic Resonance imaging (MRi) for imaging of bone and embedded metal. Both CT and MR are superior to autopsy for identification of bone injuries and trapped air [9,10].

Using CT for postmortem examinations is challenging [11]. Conditions of the body may change after death, including hydration level, and decay leading to gas production as well as degradation of structures and organs. Rigor mortis, separation, mumification, freezing and burning may complicate positioning of the body in the scanner. Contrasting this, radiation dose and motion artifacts are irrelevant in PMCT [7].

* Corresponding author. Niels Bohrs Allé 1, 5230 Odense M, Denmark.
E-mail address: peha@ucl.dk (P.L. Hansen).

https://doi.org/10.1016/j.fsisyn.2024.100478
Received 11 January 2024; Received in revised form 2 May 2024; Accepted 3 May 2024
Available online 14 May 2024

Over the last decade, several papers have been dedicated to PMCT technique, following the development of CT in general [12–15]. Often, PMCT is performed with standard settings given that the conditions of the deceased vary so much that design and choice of acquisition parameters for CT scan is cumbersome, and repetition of scans is seldom possible. In CT, visceral organs are identified based on differences in tissue density, e.g. absorption of photons, and the distinct borders between organs [16]. However, as decay increases, these distinctions become less defined, which may contribute to PMCTs inferiority to autopsy regarding identification of soft tissue lesions [9–11]. It is thus necessary to increase distinction between soft tissue organs in PMCT. Reconstruction algorithms are *in silico* tools routinely used in radiology for any data processing to modify parameters of CT images to identify organs of different mass and density [17,18].

By focusing on reconstruction algorithms instead of the acquisition parameters, reconstructions can be developed for specific aims and conditions. PMCT is still an area in development, and the multifunctional tool of reconstruction parameters including multiplanar reformat, volume rendering and different mathematical evaluations has not been fully explored. Of PMCT publications, only Gascho et al., 2018 [12] included reconstruction methods, and there are no official recommendations for PMCT reconstruction parameters.

Improved visualization of raw data in the abdominal organs is of specific interest due to rapid decay, and abdominal reconstruction protocols has previously been developed for the living [12,19].

Radio density or the ability of x-rays to penetrate a material is quantified as Hounsfield units (HU) where water is the equivalent of 0 HU, air is −1000 HU, and dense materials like bone and metal are +1000 HU [12,20]. HU levels, can be defined to focus on areas of different densities, typically depending on the anatomical area of interest [12]. A narrow range, or window, is typically chosen for distinction between soft tissues, whereas a large window is used for sharp shifts in radio density, for example the transition from soft tissue to air in the lungs. The HU scale can be extended to increase visualization of high density objects [12,21,22], but will at the same time increase visibility and decrease contrast in soft tissue. The range of the window is defined as Window Width (WW), and the central point is defined as Window Level (WL). Pre-defined built-in reconstructions in scanners are defined for living patients and do not necessarily corroborate postmortem visualization [19].

The purpose of this study was to increase distinction and identification of visceral structures in PMCT by development and exploration of a novel set of reconstruction parameters designed to postmortem conditions, to improve image quality in postmortem diagnostics. To our knowledge this is the first study to explore image quality for reconstruction parameters designed for PMCT.

2. Material and methods

2.1. Study population

For this study, we planned to include up to twenty PMCT scans performed over an eight-week period, as twenty was the maximum feasible number for grading in a visual grading analysis (VGA) due to the time that the radiologists had available. Only deceased exposed to whole body adult PMCT with fixed acquisition parameters (Table 1) could be included, thereby excluding persons below 15 years of age. Bodies in various stages of decomposition were included, and stage of decomposition was evaluated based on amount of gas formation in the soft tissues and the organ parenchyma by two independent observers. Non-decomposed were characterized by minor or no gas formation. Based on these criteria, only two bodies scanned during the acquisition period and included in the study was identified to be in severe decay by forensic pathologists.

According to Danish law, studies of pseudonymised pre-collected data do not require ethical approval. The study was registered at the University of Southern Denmark, journal no 2019–03.01-4.

Table 1
CT scan acquisition parameters for all included scans. kV: kiloVolt, mm: Millimeter, s: Seconds.

acquisition parameters	
Tube voltage	120 kV
MA RANGE	150–700
Slice thickness	1.25 mm
pitch	0.516
Rotation time	0.60 s
Noise Index	21

2.2. CT acquisition

All scans were performed on a Lightspeed VCT 64 slice scanner (GE Healthcare, Milwaukee, USA) at preset scan acquisition parameters (Table 1).

2.3. Reconstruction parameters

We compared four reconstruction parameters. One, the standard algorithm that is routinely used in PMCT is was compared with the detail algorithm provided by GE, and a novel set of two reconstruction parameters designed with the aim of increasing visibility of soft tissue structures. The standard algorithm is a blend between a soft and hard kernel, which means that the result is a combination between spatial resolution and contrast resolution. In contrast, the detail algorithm is normally used for hybrid tissue and where bone edges are important to visualize, which require a better spatial resolution and the noise is increased. This was included as it was of interest to increase enhancement of abdominal boarders [12,21–24] without adding large quantities of noise [17,25] and was therefore chosen to be tested for abdominal PMCT. The two novel reconstructions were developed based on the standard algorithm, but extending WW as suggested by Gascho et al., 2018 [12], . The novel algorithms were selected by a forensic pathologist not involved in executing the VGA and had WL of 80, and WW of 3000 and 4000, respectively, hereby bearing strong resemblances with bone window (Table 2).

Fifty percent Adaptive Statistical Iterative Reconstruction (ASiR) was used on all reconstructions as well as a Scan Field of View of 50 cm with the maximal possible display field of view (50 cm). As the area of interest was the abdomen, the reconstruction started at the superior abdominal organ and ended at the pubic symphysis.

2.4. Visual image quality assessment

All postmortem scans were analyzed with the three reconstructions novel for PMCT as well as the standard algorithm (Table 2), and resulting images were subjected to Visual Grading Analysis (VGA) by forensically trained radiologists. VGA is a scientific tool to systematically evaluated detailed perceived image quality based on anatomical structures in the images including measurements for intra- and interobserver agreement to validate the results. The 83 image sets (twenty scans with four different parameters, and three duplicated for intraobserver agreement) were assessed for six predefined image quality criteria (Table 3). As images were evaluated without a reference image,

Table 2
Parameters of the chosen reconstructions used for the VGA.

Reconstruction	Algorithm	HU WW	HU WL
1	DETAIL	350	40
2	STND	3000	80
3	STND	4000	80
4	STND	350	40

Table 3
VGA questions designed specifically for addressing increase in contrast and tissue distinction in deceased as well as presence of artifacts.

Image Criteria	Question/Subject of evaluation	Image quality parameter	Scoring
1	Homogeneity in the hepatic parenchyma	Noise	1–5
2	Sharpness of the abdominal aortic wall	Sharpness	1–5
3	Visualization of intestinal limits/ borders	Low Contrast Resolution	1–5
4	Visible difference in density between the compact and spongy bone structures in lumbar spine	Contrast	1–5
5	Streaking in pelvic region	Artifacts/Beam Hardening	1–5
6	Is the CT scan considered useful for diagnostic purpose?	Usefullness	No/Yes

it was performed as an absolute VGA [26,27]. Images were randomly mixed, blinded for scan data and including duplicates.

As there are no official internationally recognized image criteria for PMCT, five Image Criteria were created (Table 3) to correlate with the European CT image quality guidelines for abdominal CT [28]. Each image was scored on a Likert scale from one to five (Table 4), with grading criteria described in Table 4. Abdominal areas representing the five image quality criteria with the four different reconstruction parameters is depicted in Fig. 1.

Four observers, all experienced in PMCT image analysis and board-certified radiologists from Odense University Hospital, evaluated the images. The radiologists had all been responsible for assessing PMCT scans for the Department of Forensic Medicine University of Southern Denmark for approximately two years.

In addition to the first five image criteria the observers were presented with a sixth question, to evaluate whether the PMCT was useful for diagnostic purpose (Image criteria 6, Table 3).

The image sets were presented to the observers in the program Viewer for Digital Evaluation of X-ray images (ViewDex) [29]. In ViewDEX, the chosen scoring marks were displayed on the monitor and the option to return to previous scans was activated if needed. The images were in random order and blinded. The observers used a radiological workstation including a three-megapixel screen, with lighting calibrated at 410 cd/m2 (EIZO RX850, Hakusan, Japan). The screens were set after the Danish Health Authority's recommendations [30]. The radiologists were introduced to the image evaluation criteria and trained in ViewDex prior to the evaluation. A guide was handed out in paper form. Unlimited time was allowed for the evaluation, in an undisturbed room without the possibility to change WW/WL.

2.5. Statistical analysis

The analyses were performed using Stata 15 (StataCorp. 2017. Stata Statistical Software: Release 15. College Station, TX: StataCorp LLC). The VGA results of the observers were compared on each image criteria for every reconstruction using Wilcoxon matched-pairs signed-rank test. Visual Grading Analysis Score (VGAS) is the median value of all ratings of the deceased, when the numerical representations of the scale steps are used. It was performed as previously described. Mean VGAS was calculated as the mean value of VGAS of image criteria 1–5, with 95 % confidence interval (CI) and depicted as boxplot [31,32].

Inter-observer agreement was evaluated with Fleiss' kappa according to Nelson et al. [33], and intra-observer agreement was assessed using Gwet's agreement coefficient 2, chosen due to the improved chance correction compared with Cohen's kappa [34]. The intra-observer agreement was calculated based on the three duplicated reconstructions, with 1.00 being total agreement.

Table 4
VGA scores for evaluation of the image quality.

Scoring marks	Explanations
1	Inadequate, no diagnosis possible
2	Poor, diagnostic confidence substantially reduced
3	Moderate, sufficient for clinical use
4	Good, minimal limitations for clinical use
5	Excellent, no limitations for clinical use

3. Results

A total of twenty PMCT scans were included in this study. The male/female distribution of the bodies was 14/6, age range 15–84 years (IQR 41–65). Of the twenty, two were categorized as decomposed.

Answers regarding usefulness of the scans is presented overall and detailed for decomposed and non-decomposed bodies. When all scans were included, there was an overall lower positive score of image quality (89.3–95.2 %, Table 5) versus when excluding the decomposed (93.4–100 %). The reconstruction WW4000 WL80, had the lowest score, with a positive score of 89.3 % and Reconstruction1, DETAIL, was the most favorable with a positive score of 95.2 %. When excluding the decomposed bodies, DETAIL Kernel reconstruction had a 100 % and the WW4000 reconstruction WL80 had a 93.4 % acceptance rate.

Image quality was evaluated by use of the VGAS. The mean VGAS [31] for each reconstruction type were comparable, with overlapping confidence intervals (Table 6). When dividing results according to decomposition status, we found that the mean VGAS were higher for the non-decomposed bodies than for the decomposed bodies, with non-overlapping 95 % confidence intervals.

Box plot (Fig. 2) was created for all four reconstruction parameters, representing the distribution of VGA results of the five evaluation criteria noise, sharpness, low contrast resolution, contrast and artifacts/beam hardening (Table 3). The WW3000 WL80 and WW4000 WL80 reconstructions scored high, in criteria for noise, contrast, and artifacts/beam hardening, whereas DETAIL kernel and Standard scored high for the two remaining criteria, sharpness, low contrast resolution. The box plot depicts a strong pairwise comparability between the DETAIL kernel and the STND reconstruction, and between the WW3000 WL80 and the WW4000 WL80 reconstructions. When performing Wilcoxon matched-pairs signed-rank test of the image criteria, statistical disparity was found when comparing image criteria from DETAIL kernel with WW3000 WL80 ($p < 0.0001$), STND with WW3000 WL80 ($p < 0.0001$), DETAIL kernel with WW4000 WL80 ($p < 0.0001$), STND with WW4000 WL80 ($p < 0.0001$), but not when comparing DETAIL kernel with STND ($p < 1.0$), and WW3000 WL80 with the WW4000 WL80 ($p \leq 1.0$).

The inter-observer agreement analysis shows a slight to moderate agreement using the interpretation of κ values proposed by Landis and Koch [35]. The highest agreement was found at image criteria six; if the image was useful for diagnostic purpose (Table 7).

Intra-observer agreement for each of the observers was comparably high for DETAIL kernel and WW3000 WL80, but generally lower for the WW4000 WL80 reconstruction (Table 8).

4. Discussion

The aim was to improve image quality using reconstruction algorithms for PMCT scans. Four reconstructions were evaluated for diagnostic usefulness (Crit. 6) in PMCT of twenty bodies, of which two were in a state of decomposition. Scans of bodies in severe decay were evaluated less useful for diagnostic purpose than the remaining bodies, indicating that the state of the bodies severely affected image quality, and that the reconstructions could not sufficiently compensate for this. When excluding the decomposed bodies, the DETAIL reconstruction kernel scored the highest when evaluation diagnostic usefulness, whereas WW4000 WL80 scored the lowest. Interestingly, the standard reconstruction was the second best, suggesting a good diagnostic value,

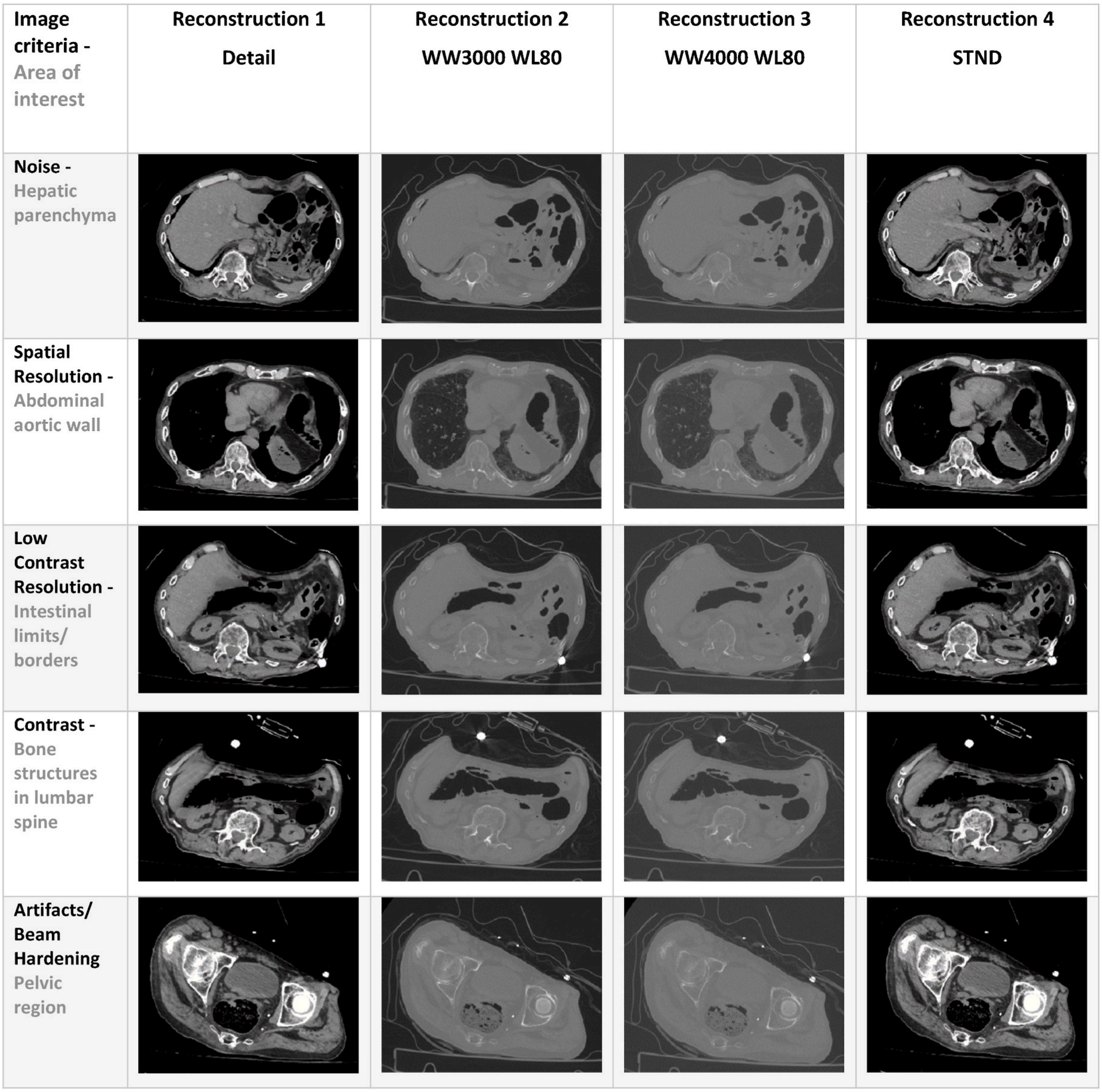

Fig. 1. Depiction of the four reconstructions and the area of interest for the different image criteria.

Table 5
Score in percent of each reconstruction type deemed useful for diagnostic purpose by the observers.

Scans	DETAIL kernel	WW3000 WL80	WW4000 WL80	STND WW 350 WL 40
A. Decomposed bodies	50 %	62.5 %	50 %	50 %
B. Non-decomposed bodies	100 %	94.7 %	93.4 %	97.4 %
C. All combined	95.2 %	91.7 %	89.3 %	91.7 %

although inferior to the DETAIL kernel.

Focusing on the VGAS the decomposed bodies scored lower than the non-decomposed across reconstruction types, indicating an overall lower satisfaction with the images of the decomposed bodies. Within the group of non-decomposed, no difference could be found across reconstruction types, with highly overlapping confidence intervals.

Further, we focused on the five image criteria (noise, sharpness, low contrast resolution, contrast, and artifacts/beam hardening) used to evaluate the reconstruction parameters. The WW3000 WL80 and WW4000 WL80 reconstructions displayed comparable distribution of results, deviating only in respect to artifacts/beam hardening, where WW3000 WL80 was superior. Similarly, a comparable pattern was observed for the DETAIL kernel and Standard reconstructions, where the

Table 6
Mean VGAS for each reconstruction with 95 % confidence interval (CI).

Scans	DETAIL kernel [95 % CI]	WW3000 WL80 [95 % CI]	WW4000 WL80 [95 % CI]	STND WW 350 WL 40 [95 % CI]
All	3.10 [2.99; 3.20]	3.15 [3.03; 3.26]	3.10 [2.99; 3.22]	3.10 [3.00; 3.21]
Decomposed bodies	2.23 [1.88; 2.57]	2.35 [1.96; 2.74]	2.18 [1.82; 2.53]	2.13 [1.77; 2.48]
Excluding decomposed bodies	3.19 [3.09; 3.30]	3.23 [3.12; 3.35]	3.21 [3.09; 3.32]	3.21 [3.11; 3.31]

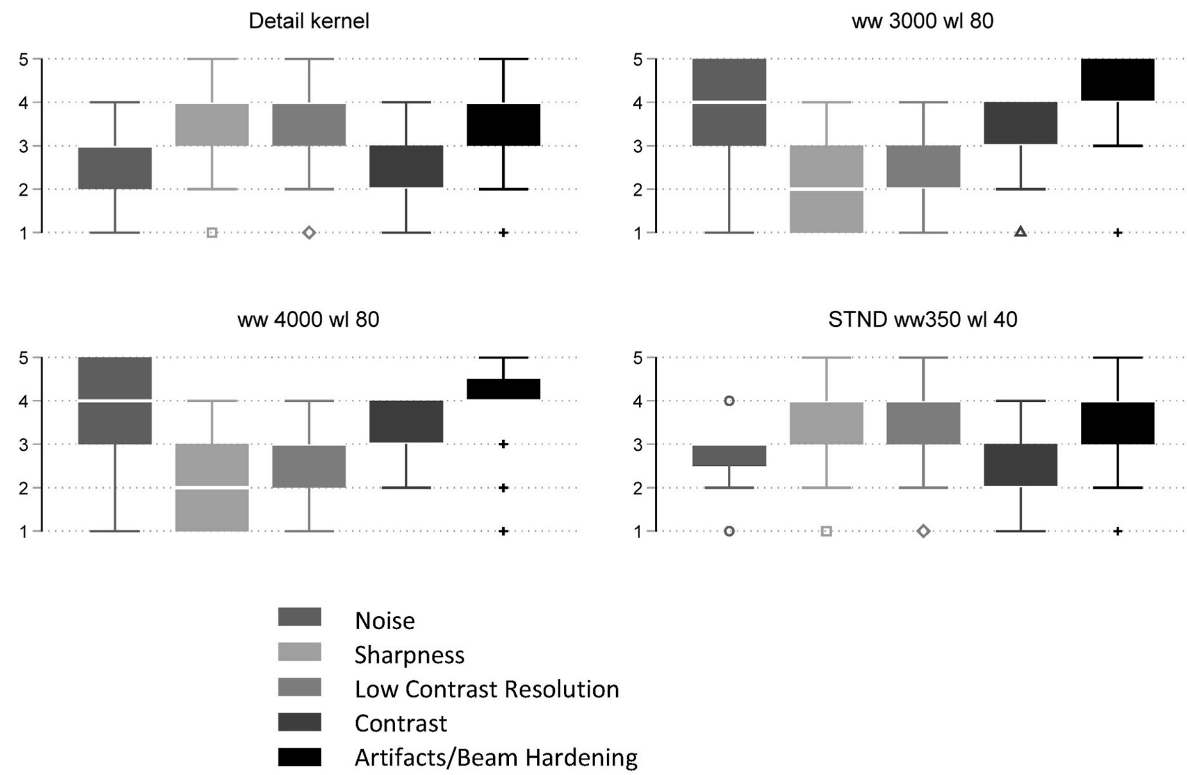

Fig. 2. Box plot of VGA results divided by reconstruction parameters.

Table 7
Inter-observer agreement in kappa for each of the IC.

Image criteria (IC)	K
1 - Noise	0.17*
2 – Spatial resolution	0.18*
3 – Low contrast resolution	0.04*
4 - Contrast	0.11*
5 – Artifacts/Beam hardening	0.14*
6 - Considered useful for diagnostic purpose	0.43**

* Marks slight agreement and ** marks moderate agreement between observers [35].

Table 8
Intra-observer agreement calculated for three image criteria based on duplicates of reconstructions using Gwet's agreement coefficient 2 with a 95 % confidence interval (CI). Values close to 1 indicates very high or complete agreement.

	DETAIL kernel, [95 % CI]	WW3000 WL80, [95 % CI]	WW4000 WL80, [95 % CI]
Noise	0.96 [0.81; 1.00]	0.93 [0.69; 1.00]	0.79 [0.70; 0.87]
Sharpness	1.00 [1.00; 1.00]	0.96 [0.81; 1.00]	0.58 [0.18; 0.97]
Low Contrast Resolution	1.00 [1.00; 1.00]	0.95 [0.78; 1.00]	0.82 [0.47; 1.00]
Contrast	1.00 [1.00; 1.00]	0.96 [0.81; 1.00]	0.89 [0.67; 1.00]
Artifacts/Beam Hardening	1.00 [1.00; 1.00]	0.96 [0.81; 1.00]	0.86 [0.62; 1.00]

primary difference was that DETAIL kernel was superior with respect to noise. The difference displayed in Fig. 2 between the DETAIL kernel and WW3000 WL80/WW4000 WL80 as well as between Standard and WW3000 WL80/WW4000 WL80 was corroborated with Wilcoxon rank test yielding a very low probability of equality. This indicates two clearly distinct groups of pairwise internally highly comparable reconstruction WW3000 WL80/WW4000 WL80 versus DETAIL kernel/Standard, with larger differences between the two groups.

For WW3000 WL80 and WW4000 WL80, the results for image criteria four—contrast—implied a good contrast between tissues with different HU levels, with the question focusing on bone structures. This was expected, as the extended HU scale enables a wider grayscale. These results were not compared with actual standard bone window settings, specifically designed to interpret bones in CT scans, and it is therefore not possible to infer whether they are different from the standard bone window setting.

WW3000 WL80 and WW4000 WL80 also scored high for the VGA criteria noise, indicating that the extended greyscale increased the visibility of hepatic structures, and for artifacts/beam hardening, which evaluates presence of artifacts in the pelvic area. The extended HU levels thus presumably changed the appearance of artifacts, as expected from earlier studies [12,19,36]. Visual representation of the WW3000 WL80 and WW4000 WL80 reconstructions displayed higher visibility of abdominal structures compared with DETAIL kernel or Standard (Fig. 1). However, this difference is not reflected in the VGA, and no firm conclusions can be made.

DETAIL kernel and Standard was superior compared to the WW3000 WL80 and WW4000 WL80 reconstructions regarding sharpness of the abdominal aortic wall and low contrast resolution seen as visualization of intestinal limits/borders. For these purposes, the narrow HU window contributed to visualize, and thereby identify the desired structures. The DETAIL kernel was not superior to the STND kernel with regards to noise, as was otherwise suggested [17,25].

Inter-observer agreement was found to be ranging from "slight agreement" to "moderate agreement", equivalent to what was found in previous studies [31]. For the intra-observer agreement, we found high correlation, indicating that the observers were consistent in their answers.

This study was the first of its kind to our knowledge, using PMCT data to evaluate a range of reconstruction setting for postmortem conditions. Although earlier publications have suggested the use of PMCT specific reconstructions [12], or applied reconstructions for analysis of PMCT scans [37,38], this is the first study systematically analyzing the usefulness of reconstructions designed for PMCT purposes.

4.1. Limitations

Preferably, the sample size of twenty would preferably have been larger, especially with regards to decomposed bodies. However, additional samples would increase time to grade the images in the VGA, beyond what was manageable by the forensic radiologists. The two decomposed bodies included, were the only ones to arrive at the institute within the timeframe of the project. The internal putrefactive state could optimal have been determined using the radiological alteration index (RAI) by a radiologist with expertise in forensic radiology, which was unfortunately not possible in this study. It would also have been of interest to further examine extension of the HU scale to increase visibility of soft tissue, also in severely decomposed bodies. However, we were not able to demonstrate this in our data. For further studies, it could be advantageous to explore further parameters in shape of different HU levels to construct window settings for different causes of death and hydration level, such as such as cases of charred bodies or bodies found in water, as well as different stages of decay. Moreover, where this study focused on the postprocessing process, a study of a combination of scan techniques with software modifications would increase the potential to improve image quality.

5. Conclusions

The study elucidates the possibility for using multiple reconstructions specialized for PMCT conditions, to accommodate the special conditions when working with deceased, which distinguishes from living patients, where the reconstructions levels are well known for different pathologies. Despite the lack of clear improvements in the tested reconstructions, this study provides an insight into some of the possibilities of improving PMCT quality using reconstruction techniques.

Funding

This research did not receive any specific grant from funding agencies in the public, commercial, or not-for-profit sectors.

CRediT authorship contribution statement

Pernille Lund Hansen: Writing – original draft, Supervision, Project administration, Methodology. **Peter Mygind Leth:** Supervision, Resources, Conceptualization. **Pernille Aagaard Nielsen:** Writing – review & editing, Visualization, Investigation, Data curation. **Dina Maria Bech:** Writing – review & editing, Visualization, Investigation, Data curation. **Julie Brandhøj Nielsen:** Writing – review & editing, Visualization, Investigation, Data curation. **Svea Deppe Mørup:** Supervision, Methodology. **Anette Koch Holst:** Investigation. **Lene Bak:** Investigation. **Mette R. Poulsen:** Investigation. **Pernille W. Greisen:** Investigation. **Dennis Lund Hansen:** Writing – review & editing, Visualization, Validation, Methodology, Formal analysis, Data curation. **Helle Precht:** Writing – review & editing, Supervision, Project administration, Conceptualization.

Declaration of competing interest

The authors declare that they have no known competing financial interests or personal relationships that could have appeared to influence the work reported in this paper.

References

[1] X. Xin, J. Shen, S. Yang, S. Liu, A. Hu, B. Zhu, et al., Improved image quality of low-dose CT combining with iterative model reconstruction algorithm for response assessment in patients after treatment of malignant tumor, Quant. Imag. Med. Surg. 8 (7) (2018) 648–657.
[2] C.W. Schmidt, CT scans: balancing health risks and medical benefits, Environ. Health Perspect. 120 (3) (2012) A118–A121.
[3] M. Mori, K. Murata, M. Takahashi, K. Shimoyama, T. Ota, R. Morita, et al., Accurate contiguous sections without breath-holding on chest CT: value of respiratory gating and ultrafast CT, AJR Am. J. Roentgenol. 162 (5) (1994) 1057–1062.
[4] W.R. Janowitz, Current status of mechanical computed tomography in cardiac imaging, Am. J. Cardiol. 88 (2a) (2001) 35e–38e.
[5] S.M. Kirchhoff, E.F. Scaparra, J. Grimm, M. Scherr, M. Graw, M.F. Reiser, et al., Postmortem computed tomography (PMCT) and autopsy in deadly gunshot wounds–a comparative study, Int. J. Leg. Med. 130 (3) (2016) 819–826.
[6] A. Moskała, K. Woźniak, P. Kluza, K. Romaszko, O. Lopatin, The importance of post-mortem computed tomography (PMCT) in confrontation with conventional forensic autopsy of victims of motorcycle accidents, Leg. Med. 18 (2016) 25–30.
[7] P.M. Leth, Computed tomography in forensic medicine, Dan Med J 62 (6) (2015).
[8] I.S. Roberts, Z.C. Traill, Use of post-mortem computed tomography during the COVID-19 pandemic, Diagn. Histopathol. 27 (10) (2021) 418–421.
[9] I. Le Blanc-Louvry, S. Thureau, C. Duval, F. Papin-Lefebvre, J. Thiebot, J.N. Dacher, et al., Post-mortem computed tomography compared to forensic autopsy findings: a French experience, Eur. Radiol. 23 (7) (2013) 1829–1835.
[10] I.S. Roberts, R.E. Benamore, E.W. Benbow, S.H. Lee, J.N. Harris, A. Jackson, et al., Post-mortem imaging as an alternative to autopsy in the diagnosis of adult deaths: a validation study, Lancet 379 (9811) (2012) 136–142.
[11] I.M. Wagensveld, B.M. Blokker, P.A. Wielopolski, N.S. Renken, G.P. Krestin, M. G. Hunink, et al., Total-body CT and MR features of postmortem change in in-hospital deaths, PLoS One 12 (9) (2017) e0185115.
[12] D. Gascho, M.J. Thali, T. Niemann, Post-mortem computed tomography: technical principles and recommended parameter settings for high-resolution imaging, Med. Sci. Law 58 (1) (2018) 70–82.
[13] P.M. Flach, D. Gascho, W. Schweitzer, T.D. Ruder, N. Berger, S.G. Ross, et al., Imaging in forensic radiology: an illustrated guide for postmortem computed tomography technique and protocols, Forensic Sci. Med. Pathol. 10 (4) (2014) 583–606.
[14] L. Filograna, N. Magarelli, A. Leone, R. Guggenberger, S. Winklhofer, M.J. Thali, et al., Value of monoenergetic dual-energy CT (DECT) for artefact reduction from metallic orthopedic implants in post-mortem studies, Skeletal Radiol. 44 (9) (2015) 1287–1294.
[15] T.D. Ruder, Y. Thali, S.A. Bolliger, S. Somaini-Mathier, M.J. Thali, G.M. Hatch, et al., Material differentiation in forensic radiology with single-source dual-energy computed tomography, Forensic Sci. Med. Pathol. 9 (2) (2013) 163–169.
[16] S.R. Manohara, S.M. Hanagodimath, L. Gerward, Energy absorption buildup factors of human organs and tissues at energies and penetration depths relevant for radiotherapy and diagnostics, J. Appl. Clin. Med. Phys. 12 (4) (2011) 3557.
[17] A. Rodriguez, F.N. Ranallo, P.F. Judy, D.S. Gierada, S.B. Fain, CT reconstruction techniques for improved accuracy of lung CT airway measurement, Med. Phys. 41 (11) (2014) 111911.
[18] R. Groell, R. Rienmueller, G.J. Schaffler, H.R. Portugaller, E. Graif, P. Willfurth, CT number variations due to different image acquisition and reconstruction parameters: a thorax phantom study, Comput. Med. Imag. Graph. 24 (2) (2000) 53–58.
[19] T.D. Ruder, Y. Thali, S.T. Schindera, S.A. Dalla Torre, W.D. Zech, M.J. Thali, et al., How reliable are Hounsfield-unit measurements in forensic radiology? Forensic Sci. Int. 220 (1–3) (2012) 219–223.
[20] L.W. Goldman, Principles of CT and CT technology, J. Nucl. Med. Technol. 35 (3) (2007) 115–128, quiz 29-128.
[21] E. Seeram, Computed Tomography: Physical Principles, Clinical Applications, and Quality Control, fourth ed.:, Elsevier, 2015, p. 576.
[22] J. Larsson, M. Båth, K. Ledenius, H. Caisander, A. Thilander-Klang, Assessment of clinical image quality in paediatric abdominal CT examinations: DEPENDENCY ON THE LEVEL OF ADAPTIVE STATISTICAL ITERATIVE RECONSTRUCTION (ASiR) AND THE TYPE OF CONVOLUTION KERNEL, Radiat. Protect. Dosim. 169 (1–4) (2016) 123–129.
[23] L.W. Goldman, Principles of CT: radiation dose and image quality, J. Nucl. Med. Technol. 35 (4) (2007) 213–225, quiz 26-8.
[24] M. Yamaguchi, H. Fujita, M. Uemura, Y. Asai, H. Wakae, M. Ishifuro, Development and evaluation of a new gray-scale test pattern to adjust gradients of thoracic CT imaging, Eur. Radiol. 14 (12) (2004) 2357–2361.
[25] J.B. Solomon, O. Christianson, E. Samei, Quantitative comparison of noise texture across CT scanners from different manufacturers, Med. Phys. 39 (10) (2012) 6048–6055.
[26] M. Båth, L.G. Månsson, Visual grading characteristics (VGC) analysis: a non-parametric rank-invariant statistical method for image quality evaluation, Br. J. Radiol. 80 (951) (2007) 169–176.
[27] F.R. Verdun, D. Racine, J.G. Ott, M.J. Tapiovaara, P. Toroi, F.O. Bochud, et al., Image quality in CT: from physical measurements to model observers, Phys. Med. 31 (8) (2015) 823–843.
[28] G. Bongartz Sjg, A.G. Jurik, M. Leonardi, E.v.P. van Meerten EUROPEAN GUIDELINES ON QUALITY CRITERIA FOR COMPUTED TOMOGRAPHY http://www.drs.dk/guidelines/ct/quality/index.htm1999 [.
[29] S. Börjesson, M. Håkansson, M. Båth, S. Kheddache, S. Svensson, A. Tingberg, et al., A software tool for increased efficiency in observer performance studies in radiology, Radiat. Protect. Dosim. 114 (1–3) (2005) 45–52.
[30] Sundhedsstyrelsen, Kontrol af monitorer til røntgen-diagnostik. https://www.sst.dk/-/media/Udgivelser/2018/Kontrol-af-monitorer-til-roentgendiagnostik.ashx?la

=da&hash=7F63392176CE7D36C8E597DE23027E57D2A046C:Sundhedsstyrelsen, 2018.
[31] C.B. Outzen, D. Maron, J. Nissen, J. Munk, L.M. Grau, D. Juhl, et al., The influence of a novel edge enhancement software on image quality of DR hand images of patients with rheumatoid arthritis, Radiography (2021).
[32] H. Precht, D.L. Hansen, B.M. Ring-Pedersen, L.F. Moller Hansen, D. Waaler, A. Tingberg, et al., Comparison of image quality in chest, hip and pelvis examinations between mobile equipment in nursing homes and static indirect radiography equipment in the hospital, Radiography 26 (2) (2020) e31–e37.
[33] K.P. Nelson, D. Edwards, Measures of agreement between many raters for ordinal classifications, Stat. Med. 34 (23) (2015) 3116–3132.
[34] D. Klein, Implementing a general framework for assessing interrater agreement in Stata, STATA J. 18 (4) (2018) 871–901.
[35] J.R. Landis, G.G. Koch, The measurement of observer agreement for categorical data, Biometrics 33 (1) (1977) 159–174.
[36] T.M. Link, W. Berning, S. Scherf, U. Joosten, A. Joist, K. Engelke, et al., CT of metal implants: reduction of artifacts using an extended CT scale technique, J. Comput. Assist. Tomogr. 24 (1) (2000) 165–172.
[37] J. Jian, L. Wan, Y. Shao, D. Zou, P. Huang, Z. Wang, et al., Postmortem chest computed tomography for the diagnosis of drowning: a feasibility study, Forensic Sci Res 6 (2) (2021) 152–158.
[38] Z. Del Fante, A. De Matteis, V. Fazio, N. Di Fazio, A. Quattrocchi, S. Romano, et al., The importance of Post Mortem Computed Tomography (PMCT) in the reconstruction of the bullet trajectory, Clin. Ter. 170 (2) (2019) e129–e133.